ASSESSING HYDROCLIMATIC DRIVERS OF GROUNDWATER FLUCTUATIONS THROUGH IOT-BASED REAL-TIME MONITORING

Yusra Riaz[1], Maham Riaz[1], Sabahat Isha[1], Khkula Falak[1], Mujahid Khan[1], Nadeem Ullah[2*], Shehryar Hassan[1]

[1]Department of Civil Engineering, University of Engineering & Technology, Peshawar, Pakistan
[2] Department of Civil Engineering, City University of Science and Information Technology, Peshawar, Pakistan
[*]Corresponding author E-mail: nadeem.ullah@cusit.edu.pk; nadeem.phdnust@gmail.com

ABSTRACT: To better understand recharge processes, groundwater depletion in semi-arid regions experiencing increasing development needs ongoing monitoring. This study examines the role of hydroclimatic factors in regulating groundwater level variations on a short timescale and assesses the efficacy of a low-cost Internet of Things (IoT) network for groundwater level monitoring in a managed aquifer recharge (MAR) well in Islamabad, Pakistan. Strong agreement (R^2 = 0.998) was found when the system was calibrated and validated in the lab against a commercial water level data recorder. In addition to satellite-based meteorological data, daily data from December 2023 to April 2024 contained temperature, total dissolved solids (TDS), and groundwater level. The analysis of the data reveals that atmospheric demand primarily regulates the groundwater system, particularly during the dry season. This is demonstrated by the positive correlations between groundwater level and air temperature (r = 0.68) and ET0 (r = 0.70), whereas precipitation is a response with a lag. Simplified groundwater balance models are inadequate, as evidenced by the weekly water balance's only 2% variability. The need for thorough water quality monitoring is highlighted by the high total dissolved solids (TDS) concentration values (2,300–3,900 mg/L). The study proves the effectiveness of IoT-based systems for real-time MAR performance evaluation in data-poor urban areas.

Keywords: *Groundwater monitoring; Managed aquifer recharge (MAR); Internet of Things; Precipitation; Evapotranspiration; Urban groundwater; TDS; Water table fluctuation.*

INTRODUCTION

Groundwater represents about 30% of the world's freshwater and is the main drinking water source for about 2.5 billion people globally (Famiglietti, 2014; United Nations, 2022). Groundwater is particularly important in arid and semi-arid areas, where the availability of surface water is low and seasonally fluctuating. Currently, groundwater abstraction worldwide is estimated at about 982 km³ per year, making it the most abstracted raw material on the planet (NGWA, 2024). About 70% of this abstraction is used for agricultural irrigation, while about 38% of the world's irrigated agricultural land uses groundwater as its main water source (United Nations, 2022).

Groundwater is a critical resource, but it is increasingly being subjected to the pressures of growing population, urbanization, agriculture just depleting more water, and the changing climate (Gorelick and Zheng, 2015; Green *et al*., 2011). The difference between how much we are extracting and how much nature can recharge has resulted in many aquifers going downhill, causing land to sink, saltwater intrusion, and deteriorating water quality (Famiglietti, 2014). The IPCC findings and projections indicate that surface and groundwater resources are susceptible to climate variability, with about 20% of the increase in global water scarcity being attributed to hydroclimate change (Sophocleous, 2004; Bates *et al*., 2008).

Pakistan is the fourth-largest consumer of groundwater resources globally, abstracting approximately 64.82 km³ annually, with a staggering 94% of this abstracted for irrigation (Qureshi, 2020). Approximately 1.2 million private tubewells exist nationwide, with the Punjab province housing 85% of them. These tubewells are rapidly surpassing the pace of natural recharge in terms of groundwater abstraction (Qureshi, 2020; Razzaq *et al*., 2022). One of the world's most overstretched aquifers is the Indus Basin aquifer, which lies beneath a significant amount of the nation's agricultural area (Qureshi *et al*., 2008). For 60–70% of Pakistan's population, groundwater is their sole source of survival (IAH, 2017). However, there is a troubling gap in this regard: there is no national groundwater monitoring program in existence, and there is no systematic monitoring (Bhatti *et al*., 2017).

Islamabad, the capital of Pakistan, is at the intersection of rapid urbanization and groundwater depletion. Located on the Potohar Plateau, 500-700 meters above sea level, and nestled in the foothills of the Margalla Hills, the city spans approximately 906 square kilometers, with a complex underground profile that includes "multi-layer aquifers of gravel and boulders, alternating with clay

DOI: https://doi.org/10.57041/f3yffx28

and shale deposits," as observed in studies such as Iqbal *et al*. (2023). Despite receiving an average annual rainfall of 1500 mm, the groundwater level has drastically fallen by as much as 85 feet between 2013 and 2017, according to Jadoon *et al*. (2023). Several factors are contributing to this situation. The city's population has broken the two-million mark with an average annual growth rate of 5.7%. The Capital Development Authority (CDA) operates some 200 tubewells to provide the city's water requirements (Jadoon *et al*. 2023), while in the peri-urban areas, unregulated private borewell installations continue to deplete the same groundwater resource (Iqbal *et al*. 2023). This has created a situation where the city's daily water requirement exceeds 475 million liters, although the supply does not go beyond 280 million liters.

To combat the reduction in groundwater, the CDA collaborated with the Pakistan Council of Research in Water Resources (PCRWR) to introduce managed aquifer recharge (MAR) wells in Islamabad in 2022 (Arshad *et al*., 2023; Iqbal *et al*., 2023). MAR is a strategic approach to recharge aquifers by harnessing various water sources such as rainwater, stormwater, and treated effluent. Currently, the annual use of MAR worldwide is increasing at a rate of 5% each year, amounting to approximately 10 km^3 of recharged water per annum (Dillon *et al*., 2019; Zhang *et al*., 2020). However, in order to evaluate the process's success, MAR relies on ongoing monitoring of groundwater levels and water quality (Dillon, 2005).

Chalked tape measures, electronic water level recorders, and data loggers, including HOBO sensors, are used in the traditional method of groundwater observation on a regular basis. The quick recharging process and the post-rainfall reaction to rainfall events are not captured by this method, which is very expensive and time-consuming and yields scarce data, usually before and after the monsoon season in Pakistan (Condon *et al*., 2021; Bhatti *et al*., 2017). With the advent of IoT technology, real-time, continuous, and affordable groundwater observation is now feasible using IoT-based systems that incorporate low-cost sensors, microcontrollers, and wireless communication. These technologies allow for more dynamic groundwater resource management by transmitting data on a variety of groundwater parameters at a high frequency (Jadoon *et al*., 2023).

Effective management of aquifer resources requires an understanding of how hydroclimatic phenomena and groundwater flow dynamics interact. Previous studies have used artificial neural networks (ANN) in the Ravi-Sutlej interfluve of Punjab, Pakistan (Iqbal *et al*., 2020) and the measurement of long-term monsoonal rainfall patterns at multiple locations (Daliakopoulos *et al*., 2005) to identify rainfall as the primary driver of groundwater level fluctuations. However, these studies relied on conventional groundwater monitoring data with coarse temporal resolution and did not account for the real-time response of Managed Aquifer Recharge (MAR) wells to specific weather events. Moreover, evapotranspiration (ET), the total loss of water from the soil and vegetation to the atmosphere, is an important, yet frequently overlooked, process influencing the net rate of groundwater recharge. This is particularly important in semi-arid climates where ET rates can approach or even exceed rainfall amounts during extended drought periods (Wu *et al*., 2020; Todd and Mays, 2005). Projections of climate change suggest that increased temperatures will lead to higher potential ET rates, potentially offsetting the effects of sustained or increased rainfall on net groundwater recharge (Green *et al*., 2011; Wu *et al*., 2020).

This research addresses the existing gaps in groundwater monitoring by deploying and testing a low-cost Internet of Things (IoT) system in a managed aquifer recharge (MAR) well, and by utilizing groundwater, water quality, and meteorological data. Despite the growing usage of IoT devices for groundwater monitoring, the majority of previous research has been on regional-scale studies with limited temporal resolution or long-term trend analysis. There is currently little high-resolution MAR system monitoring in semi-arid urban regions. Furthermore, it is unclear how short-term hydroclimatic forcing affects groundwater level variability, particularly the relative significance of evapotranspiration-driven losses vs recharge delays. The objectives of the study include (i) calibrating and validating the IoT-based smart groundwater level monitoring system against a commercial HOBO water level sensor, (ii) tracking changes in a MAR well's groundwater level to ascertain its response to rainfall events, and (iii) examining the relationship between precipitation, reference evapotranspiration, and groundwater level variations.

MATERIALS AND METHODS

Study Area: The study is situated in Sector H-10, Islamabad, Pakistan, which is tucked away at the base of the Margalla Hills on the Potohar Plateau (33.66°N, 73.02°E). The Islamabad Capital Territory covers approximately 906 square kilometers, ranging from 500 to 700 meters above mean sea level, with a highest point of approximately 1493 meters in the Margalla Hills (Iqbal *et al*., 2023). The area is topographically very rugged, with numerous ridges and valleys formed mainly by the alluvial deposits eroded from the Margalla Hills.

DOI: https://doi.org/10.57041/f3yffx28

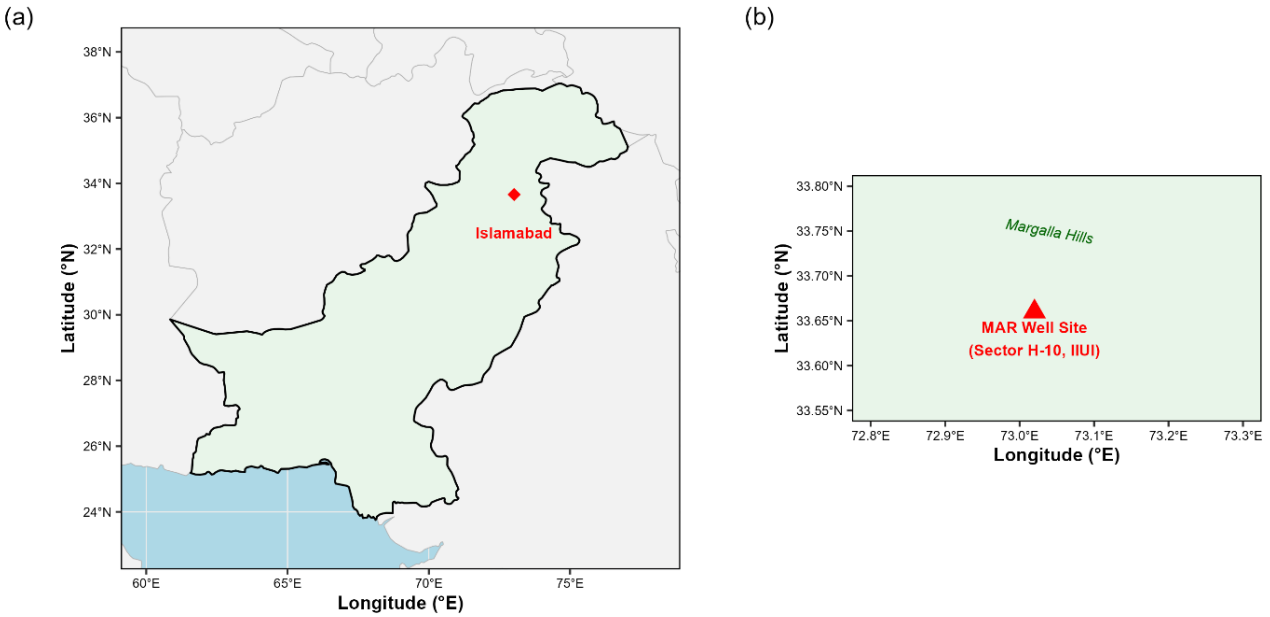

Figure 1: Study Area Map Showing the MAR Well Site Coordinates in the Study Area

The groundwater system in the study area is complex and stratified. In the upper layers, attempts by rainfall and seepage from the streams to infiltrate are largely hindered by the clayey deposits, with very little sand in the upper layers. Below this, the groundwater is confined in layers of gravel and boulders of varying thickness, layered with deposits of clay and shale. Recharge of the groundwater occurs largely through rainfall that seeps into the base of the Margalla Hills, recharging the groundwater that supports the regions downstream (Iqbal *et al*., 2023).

Managed Aquifer Recharge (MAR) Well Description: A monitoring system is installed at a specially designed mixed-use groundwater well at the International Islamic University, Islamabad (IIUI), in Sector H-10. The groundwater well is linked to a water collection tank that is 2.44 m by 2.44 m in size at the top and 2.44 m deep (8 ft by 8 ft and 8 ft deep). The water collection tank has a three-layer filtration system with a combination of different-sized gravel to treat the storm water and rainwater before it is channeled into the recharge groundwater well. This groundwater well is only used for recharge purposes and does not have a pumping system.

IoT-Based Smart Groundwater Monitoring System: The proposed work adopts a low-cost smart groundwater monitoring system designed by Jadoon *et al*. (2023). The system is centered on an Arduino Mega board with sensors and communication interfaces. The key components include a piezometric pressure sensor, a TDS and temperature sensor (DS18B20), GSM module (for wireless data communication for remote monitoring), a Real-Time Clock (RTC) module, SD card module, an OLED display, a relay module and a power supply (a 12V battery that is regulated to 5V and 3.3V using voltage regulators, with solar panel recharge capability).

The system was programmed to read the sensor values every 30 minutes, storing the values in the SD card as well as transmitting them to the remote server using the GSM module. To provide a reliable means of transmitting the data, multiple communication channels were established (Jadoon *et al*., 2023).

Laboratory Calibration: We calibrated the piezometric sensor in the lab before deploying the device in the field. A vertical water column filled to 180 cm height and measuring 200 cm in height with an inner diameter of 15 cm was used. Next, we measured the voltage shown on the OLED display at each depth as we dropped the sensor 10 cm from the top to the bottom. We found a linear relationship between depth and voltage that could be written as

$$d = mV + c \qquad (1)$$

where V stands for the sensor voltage (V), m for the slope, c for the intercept, and d for depth (cm). To correct for a systematic inaccuracy, the value of the intercept was then added to the Arduino code. To make sure that the residual errors were nearly nil, this calibration was done again.

We ran both systems concurrently on the same calibration column, the piezometric sensor, and a HOBO U20L-04 water level recorder to confirm the smart system's accuracy in comparison to the industry standard. Over the course of twenty-five minutes, the column was filled and emptied to cycle the water level.

DOI: https://doi.org/10.57041/f3yffx28

Field Installation and Data Acquisition: After the calibration process was finished in the lab, we installed the monitoring system in the MAR well at Sector H-10, Islamabad, towards the end of November 2023. The piezometric level sensor was lowered on a cable to the water table, with the sensor head just below the groundwater level. The temperature and TDS sensors were placed at the same water table level. At the top of the well head was a weatherproof box that housed the Arduino board, GSM module, RTC clock, SD card, relay, and OLED display. A solar panel installed near the well ensured that the 12V battery remained charged.

The continuous data collection started on December 5, 2023, and ended on April 15, 2024, providing us with a total of 132 days of data collection. The sensor data was collected more frequently than on an hourly basis, and we obtained daily averages of groundwater level (ft), TDS (mg/L), and temperature (°C). There is a gap in the data from February 4 to February 15, 2024, due to a power failure that was temporarily addressed by replacing the solar charge controller. There is also a gap in the data from April 3-5, 2024, due to a maintenance visit.

Hydroclimatic Data: We extracted daily meteorological data for the period of interest from the NASA POWER (Prediction of Worldwide Energy Resources) database by specifying the location coordinates 33.66°N, 73.02°E (https://power.larc.nasa.gov). The data set provides precipitation (mm/day), mean air temperature (°C), daily maximum and minimum temperatures (°C), relative humidity (%), wind speed at 2 m (m/s), and solar incoming radiation. The data offers dependable geographical and temporal coverage, which is advantageous for correlation analysis in regions with little gauge coverage, even if satellite-based precipitation products may exhibit biases when verified against gauge readings (Iqbal *et al*., 2023). The daily precipitation amounts are directly obtained from NASA POWER. Reference evapotranspiration (ET_0) was determined using the Penman equation (Penman, 1948). It is expressed by the following equation:

$$ET_o = \frac{AH + \alpha E_a}{A + \alpha} \qquad (2)$$

In this equation, ET_0 is expressed in millimeters per day. The constants are α, the psychrometric constant (0.49 mm Hg/°C); A, the slope of the saturation vapor pressure-temperature curve (mm Hg/°C); H, the net radiation (in mm of water per day); and Ea, the drying power of the air (mm/day). Ea is calculated as:

$$E_a = 0.00218 \times (160 + u_2) \times (e_s - e_a) \qquad (3)$$

In this, u_2 is the mean wind speed at 2 meters height (km/day); es is the saturation vapor pressure at the mean air temperature (mm Hg); and ea is the actual vapor pressure (mm Hg). The net radiation H is calculated using the Penman radiation formula, which takes into account the extraterrestrial radiation, actual sunshine duration, surface albedo (assumed to be r = 0.2 for grass), and the Stefan-Boltzmann long-wave radiation correction (Todd and Mays, 2005).

Table 1: Data used in the Current Study

Sr No	Data Type	Variable used	Temporal Resolution	Source
1	Groundwater	Depth	Daily	IoT-based monitoring
2		TDS	Daily	IoT-based monitoring
3		Temperature	Daily	IoT-based monitoring
4	Meteorological	Precipitation	Daily	NASA Prediction of Worldwide Energy Resources (POWER) database
5		Air Temperature	Daily	NASA Prediction of Worldwide Energy Resources (POWER) database
6		Relative Humidity	Daily	NASA Prediction of Worldwide Energy Resources (POWER) database
7		Wind Speed	Daily	NASA Prediction of Worldwide Energy Resources (POWER) database

Data Analysis: All the analysis is done in R-studio and plots are generated for each variable/scenario. Descriptive statistics (mean, standard deviation, minimum, maximum, and range) were calculated for all observed parameters during the study period and monthly. To investigate changes in water quality and potential dilution reactions associated with recharge events, the temporal history of total dissolved solids (TDS) was examined.

Pearson correlation analysis: Pearson correlation coefficients (r) were calculated between groundwater level and each hydroclimatic variable (precipitation and ET0) at daily and weekly time resolutions. The results were tested for significance at the $p < 0.05$ and $p < 0.01$ significance levels.

Lag-correlation analysis: Cross-correlation functions were calculated to identify the time lag (in days) at which precipitation affects the groundwater level most significantly. This time lag reflects the travel time of infiltrated water from the vadose zone to the water table

DOI: https://doi.org/10.57041/f3yffx28

and gives information about the recharge response of the aquifer.

Simplified water balance: A weekly net water input (NWI) was introduced as:

$$NWI = P - ET_o \quad (4)$$

where P is the weekly cumulative precipitation, and ET_0 is the weekly cumulative reference evapotranspiration. The weekly mean groundwater level change (ΔGW) was then regressed on NWI to test the explanatory power of the hydroclimatic water balance on observed groundwater level changes.

RESULTS

Sensor Calibration and Validation: After the piezometric sensor was calibrated in a lab, the voltage output of the sensor and the observed water depth were shown to have a strong linear relationship:

$$d = 87.36V - 94.8 \quad (5)$$

where V is the voltage in volts and d is the depth in centimeters (see Figure 2). Excellent linear performance is demonstrated by the coefficient of determination (R^2 = 0.9992) over the whole measured range of 0-180 cm. Systematic errors were reduced to almost zero values for every calibration point once the calibration offset (intercept correction of -94.8) was applied to the Arduino code.

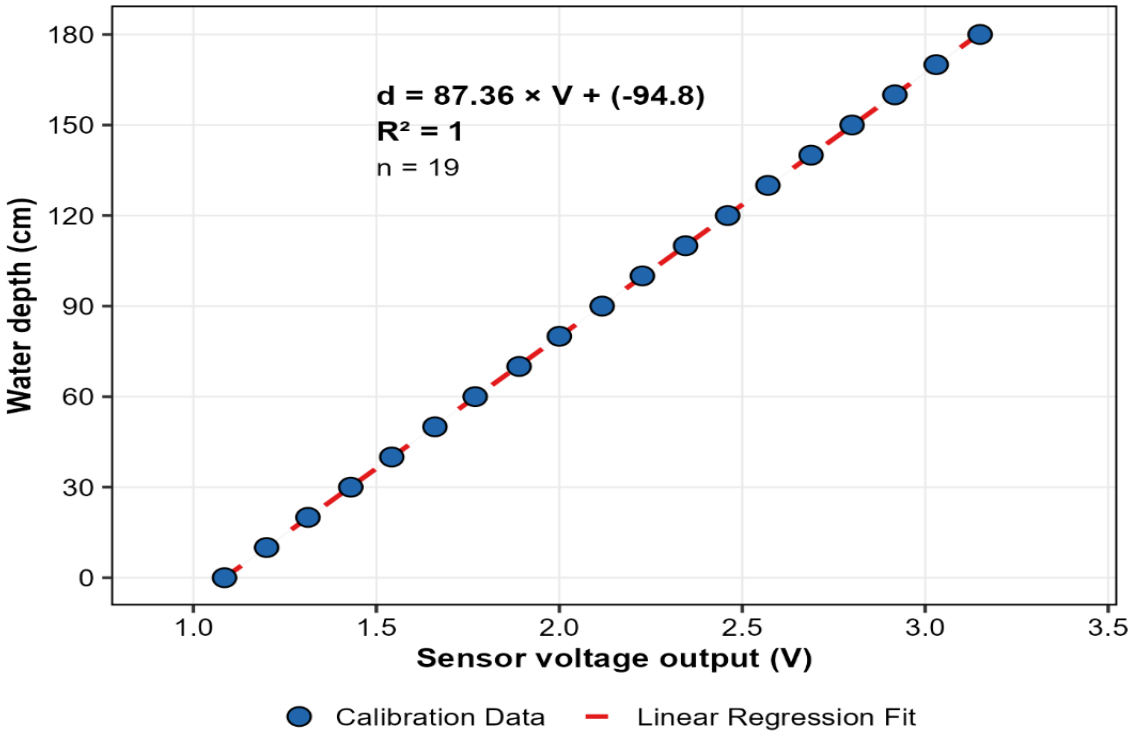

Figure 2: Scatter Plot of Measured Depth (cm) versus Sensor Voltage (V) with Linear Regression Line

During a 25-minute filling and draining cycle, the HOBO U20L water level recorder was used to verify the IoT smart system's performance in the dynamic validation test. Strong agreement between the two systems was demonstrated by the results (Figure 3). The smart system accurately tracked the HOBO reference over a depth range of roughly 50–280 cm, with a mean absolute error (MAE) of 2.23 cm, a root mean square error (RMSE) of 2.83 cm, a coefficient of determination (R^2) of 0.9982, and a Nash-Sutcliffe Efficiency (NSE) of 0.9981. The low-cost IoT piezometric sensor offers measurement accuracy comparable to the commercial reference system, as demonstrated by the residuals, which were dispersed randomly around zero without systematic bias.

Temporal Variations of Groundwater Depth: The 132-day groundwater depth data, collected using the IoT network from December 5, 2023, to April 15, 2024, is presented in Figure 4 (multi-panel). During the initial phase of groundwater monitoring (December 5-12, 2023), the groundwater depth was relatively constant at around 58.0 ft, reflecting the pre-recharge conditions. A strong and sudden decrease in groundwater depth (or a rise in the water table) of about 4.2 ft was observed between December 12 and December 13, with the depth reducing from ~58.0 ft to ~53.8 ft (Figure 4a). This corresponds to

DOI: https://doi.org/10.57041/f3yffx28

the start of the MAR well operation and represents the onset of the first recharge pulse at the sensor level, and not a reaction to a precipitation event, as no major precipitation was recorded during this period (Figure 4b).

After the initial period of adjustment due to the recharge process, the groundwater level showed a gradual and mostly monotonic decrease, from around 53.8 ft in mid-December to about 57.0-57.2 ft in mid-April. This represents a cumulative decline of the water table by about 3.2 ft during the period following the commissioning of the site. The 7-day moving average smooths out the fluctuations and highlights the general seasonal pattern, which reflects the transition from the post-monsoon recharge recovery phase to the dry, pre-monsoon season characterized by lower precipitation recharge and higher evapotranspiration rates.

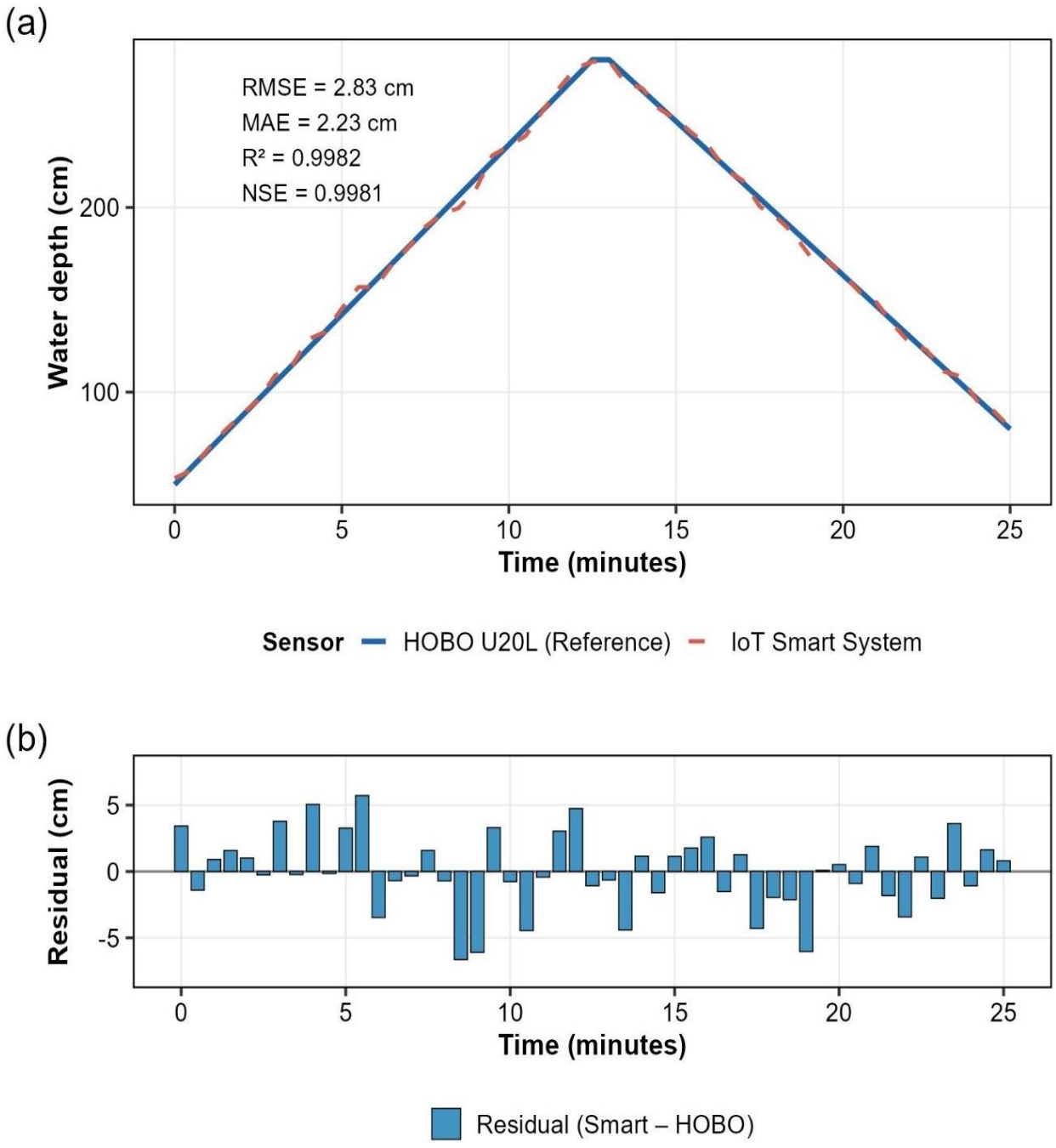

Figure 3: Time-Series Overlay Plot of Water Depth (cm) Measured Concurrently by the HOBO U20L Sensor (Solid Blue Line) and the IoT Smart System (Dashed Red Line) Throughout the Validation Experiment in the Lab

DOI: https://doi.org/10.57041/f3yffx28

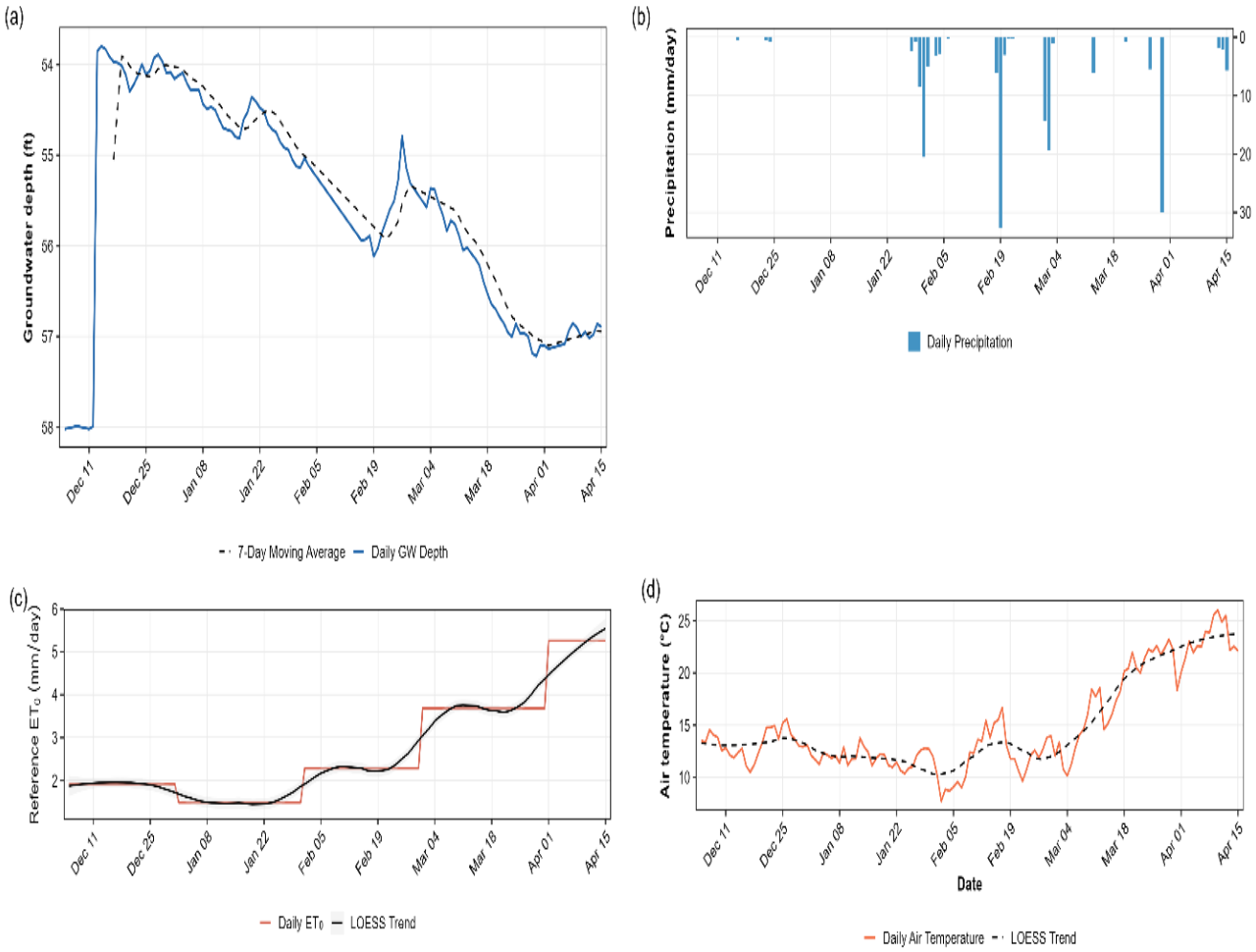

Figure 4: Multi-Panel Time Series of Monitored and Hydroclimatic Variables: (a) Daily Groundwater Depth with 7-Day Moving Average; (b) Daily Precipitation (mm/day); (c) Daily Reference Evapotranspiration ET_0 (mm/day) with LOESS Trend; (d) Daily Mean Air Temperature (°C) with LOESS Trend

The precipitation events shown in Figure 4b are linked to a number of points of interest in the short-term record that diverge from the overall trend of groundwater level drop.

- Late January episode (around January 18-22): The deepening process temporarily paused and reversed during which a sequence of precipitation events with cumulative totals of 5–10 mm/day occurred. The groundwater depth decreased from around 54.8 feet to 54.4 feet before continuing its downward trajectory.
- Mid-February response (about February 18–25): The greatest precipitation event set off the strongest groundwater response, which peaked on February 19 at a daily rate of 30 mm/day (Figure 5b). In roughly five to seven days, the groundwater depth decreased from roughly 56.1 feet to 54.8 feet, indicating a 1.3-foot rise in the water table. This is the biggest single recharge-induced fluctuation that was observed throughout the research period.
- Early March response (around March 1-5): A second major precipitation event with totals of 10-15 mm/day over several consecutive days caused a noticeable water-table increase of 0.5-0.8 ft, temporarily halting the deepening process.
- Late March Stabilization (around March 25): Although there was a significant event of precipitation (~30 mm/day around April 1), the effect on the groundwater was significantly reduced compared to the February event. The depth of the water table remained close to 57.0 ft, with a slight decrease, which indicated that with the increase in the depth of the water table, the thickness of the unsaturated zone also increased.

The environment in which groundwater activities are immersed is provided by the multi-panel time series (Figure 4, panels c and d). According to the LOESS (Locally Estimated Scatterplot Smoothing) trend (Figure 4c), the reference evapotranspiration (ET_0) increases significantly from around 1.9 mm d^{-1} in December to 5.0–

DOI: https://doi.org/10.57041/f3yffx28

5.5 mm d^{-1} in mid-April. The primary source of this value's roughly threefold increase during the season is the rise in air temperatures, which go from 10–14°C in December–January to 20–25°C in March–April (Figure 5d). Beginning in late February and lasting through April—the time of the fastest groundwater deepening—the LOESS fit to the air temperature series shows a significant rise.

Correlation Between Groundwater Depth and Hydroclimatic Variables

Daily-Scale Correlations: The correlation matrix heatmap (Figure 5) displays the Pearson correlation analysis of the daily groundwater depth and the collection of hydroclimatic and water quality factors. The findings show a complicated but physically sound pattern of correlations between the variables.

The strongest and most favorable correlation between reference evapotranspiration and groundwater depth ($r = 0.70$, $p < 0.001$) indicates that when ET_0 values rise, groundwater depth rises as well (i.e., the water table falls). As expected, given that temperature is the primary regulator of ET_0 and that the two variables have a substantial correlation ($r = 0.84$, $p < 0.001$), air temperature also exhibits a strong and positive correlation ($r = 0.68$, $p < 0.001$). These correlations are in line with the three variables' primary seasonal covariation, which states that the recharge deficit and water table depth increase as winter and spring temperatures and evapotranspiration rise.

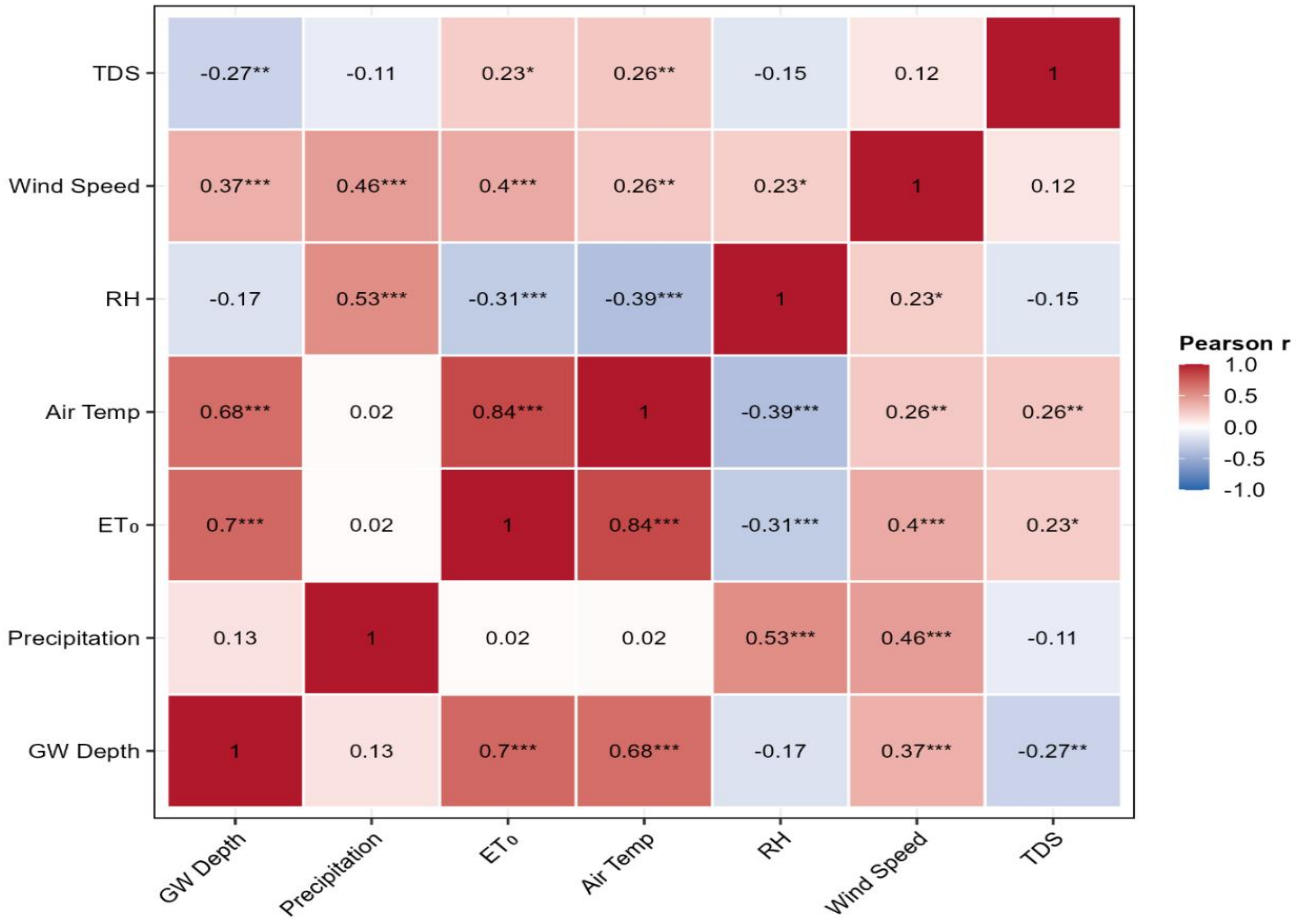

Figure 5: Pearson Correlation Matrix Heatmap for all Monitored and Derived Variables

*Note: Significance levels are indicated by asterisks: *p < 0.05, **p < 0.01, ***p < 0.001. Color intensity indicates correlation strength (red = positive, blue = negative).*

Conversely, the correlation between precipitation and groundwater level on a daily timescale was weak and not statistically significant ($r = 0.133$, $p = 0.162$. While this result appears to contradict expectations, it can be explained physically by two considerations. Firstly, the time delay between a precipitation event and the corresponding groundwater response, which is of the order of 7 days as suggested by the lag analysis (Section 3.4), weakens the correlation on a daily timescale. Secondly, the strong seasonal trend in groundwater level, which is a systematic deepening, can be considered a confounding factor, as most of the larger precipitation events occurred

DOI: https://doi.org/10.57041/f3yffx28

in February and March when the groundwater level was already much deeper than in December, such that larger precipitation values were accompanied by larger groundwater depths in the raw time series.

Precipitation was found to have a moderate positive correlation with relative humidity ($r = 0.53$, $p < 0.001$) and wind speed ($r = 0.46$, $p < 0.001$) on a daily time scale, but no association with reference evapotranspiration (ET_0; $r = 0.02$, $p > 0.05$) and air temperature ($r = 0.02$, $p > 0.05$) (Figure 6). These results suggest that the precipitation occurrences in the study region during the period of interest were not associated with temperature-controlled seasonal cycles; rather, they were associated with synoptic-scale meteorological disturbances, known as western disturbances, which bring moisture and wind, and are not controlled by the seasonal temperature cycle.

Lag-Correlation Analysis: The result of the lag correlation analysis (Figure 6) is an examination of the Pearson correlation between precipitation and the change in groundwater depth (ΔGW) at increasingly larger time lags from 0 to 14 days. The correlogram shows a clear cycle with a strong negative correlation at a 7-day time lag ($r = –0.474$). This result shows that, on average, the maximum increase in the water table (negative ΔGW, or depth increase) occurs seven days after a precipitation event.

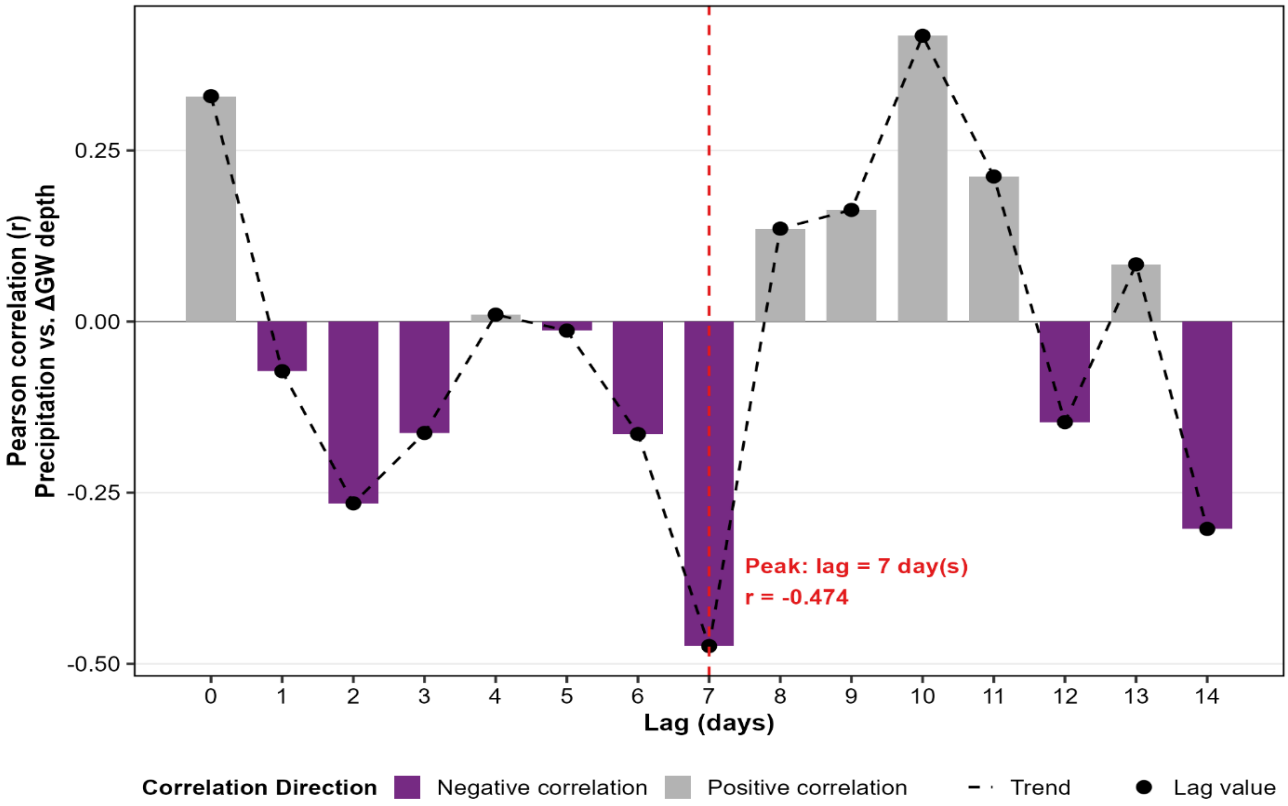

Figure 6: Lag-Correlogram Showing Pearson Correlation Coefficients Between Daily Precipitation and Daily Change in Groundwater Depth (ΔGW) at Lags of 0 to 14 Days.

Note: Purple bars indicate negative correlations (precipitation leads to water table rise); grey bars indicate positive correlations

The correlogram further shows a secondary set of negative correlations at shorter time lags (2-3 days, $r \approx –0.15$ to $–0.27$) and a negative correlation at the 14-day time lag ($r \approx –0.27$), indicating a complex, multi-modal recharge process. The positive correlations at intermediate time lags (8-11 days, peaking at $r \approx 0.35$ at the 10-day time lag) are probably indicative of a rebound effect, where the water table starts to recede as the initial recharge-induced increase has passed. The peak negative correlation ($r = –0.474$) occurs at a lag of 7 days, indicating that the maximum water table rise in response to precipitation occurs approximately one week after the rainfall event. This 7-day lag is consistent with previous studies of recharge processes in semi-arid alluvial aquifer systems, where the vadose zone thicknesses of 15-20 m (approximately 50-60 ft, as is the case at the study site) result in large transit-time delays (Sophocleous, 2004; Green *et al*., 2011).

DOI: https://doi.org/10.57041/f3yffx28

Water Balance Analysis: The relationship between weekly changes in groundwater depth (ΔGW) and weekly net water input (NWI = P – ET_0) is shown in Figure 7. The regression equation is:

$$\Delta GW = 0.0078 \times NWI \times 0.007 \quad (6)$$

With R^2 = 0.02, p = 0.59, and n = 17 weekly observations, the regression line has a very small positive slope that is not statistically significant (p = 0.59). This shows that there is no linear relationship between the weekly net water input (NWI) and the weekly changes in groundwater depth (ΔGW) at this site. The R^2 value of 0.02 is remarkably low, and this shows that the NWI explains only 2% of the variance in the ΔGW, and other factors, such as lateral groundwater flow, recharge that takes a long time to reach the groundwater due to the thick vadose zone, or regional aquifer processes, may be dominating the groundwater response at this site.

The data points shown in Figure 8 are distributed in both the "ET0 > P / GW rising" and "P > ET0 / GW declining" quadrants. It is important to note that the periods of strongly positive Net Water Imbalance (NWI; P > ET0, up to about +25 mm) and those of positive changes in groundwater (ΔGW) with a declining water table, as well as periods of negative NWI with a rising water table, seem counterintuitive. The data points are mostly concentrated in the negative NWI region (NWI < 0), which is in line with the evapotranspiration-dominated conditions during the winter-spring dry season at the study site. There is one data point that stands out as a strong outlier, indicating a weekly ΔGW of about -3.5 ft for moderately negative NWI conditions, which is likely to represent the abrupt initial adjustment process in December.

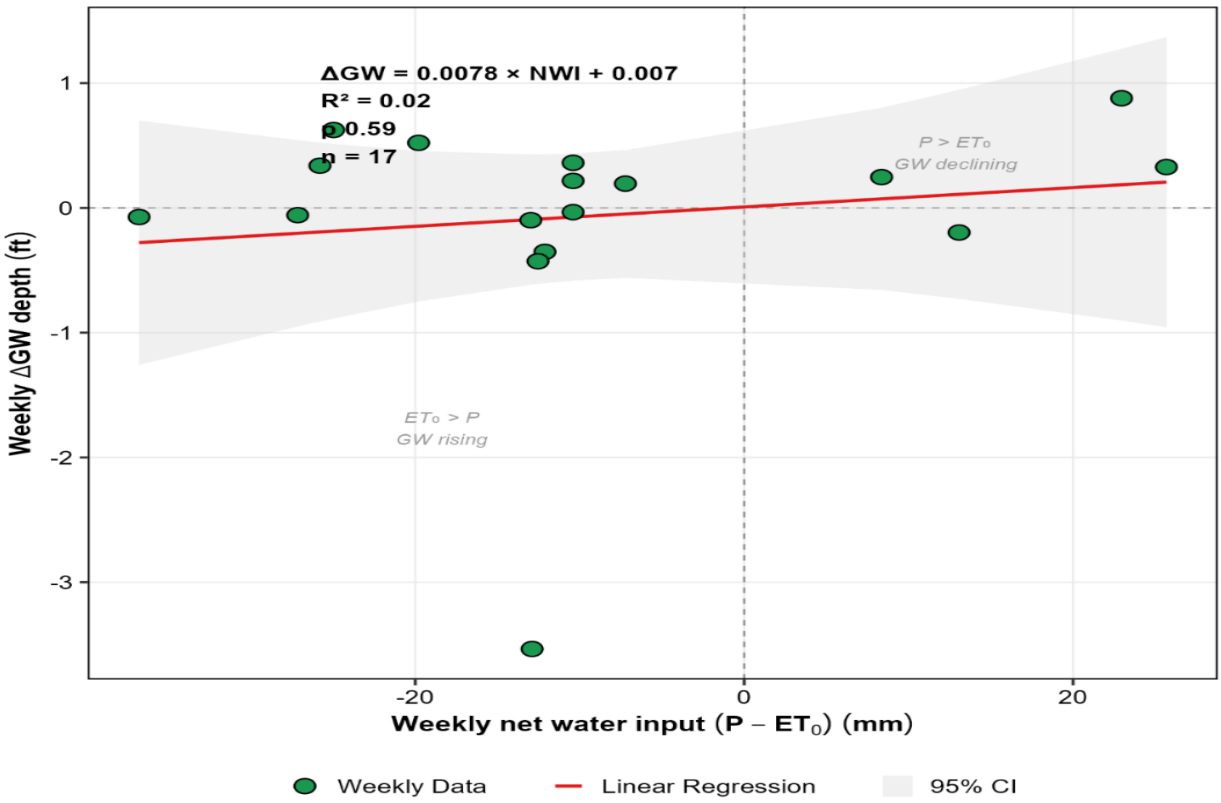

Figure 7: Weekly Change in Groundwater Depth (ΔGW) as a Function of Weekly Net Water Input (NWI = P – ET_0) During the Monitoring Period (December 2023 – April 2024).

Note: The red line shows the linear regression, and the grey shaded region represents the 95% confidence interval.

Cumulative Water Balance: The cumulative water balance analysis (Figure 8) offers a synoptic view of the precipitation inputs and evapotranspiration losses over the entire period of the study. During the period of the study, the accumulated evapotranspiration (ET_0) values exceeded the accumulated precipitation values (Figure 8a), with the deficit increasing steadily from December to April. The accumulated ET_0 increased linearly from December to January, followed by a sharp acceleration from March onwards as the temperature and solar radiation inputs increased. In contrast, the total precipitation stayed at zero until the middle of January, after which it gradually increased to reflect the individual storm events that occurred in late January, mid-February, and early March.

DOI: https://doi.org/10.57041/f3yffx28

The cumulative net water input (NWI) measurements (Figure 8b) demonstrate a steady decrease over the course of the study, and the NWI is always negative. From December to late January, the cumulative NWI gradually decreased to around -90 mm. It then partially recovered during the precipitation-dominated periods from late January to early March, briefly rising to roughly -50 mm in early March. However, the acceleration of evapotranspiration (ET_2) rates over precipitation causes the cumulative NWI to sharply decline starting in mid-March, reaching roughly -180 mm by mid-April. This is in line with the groundwater level rising concurrently.

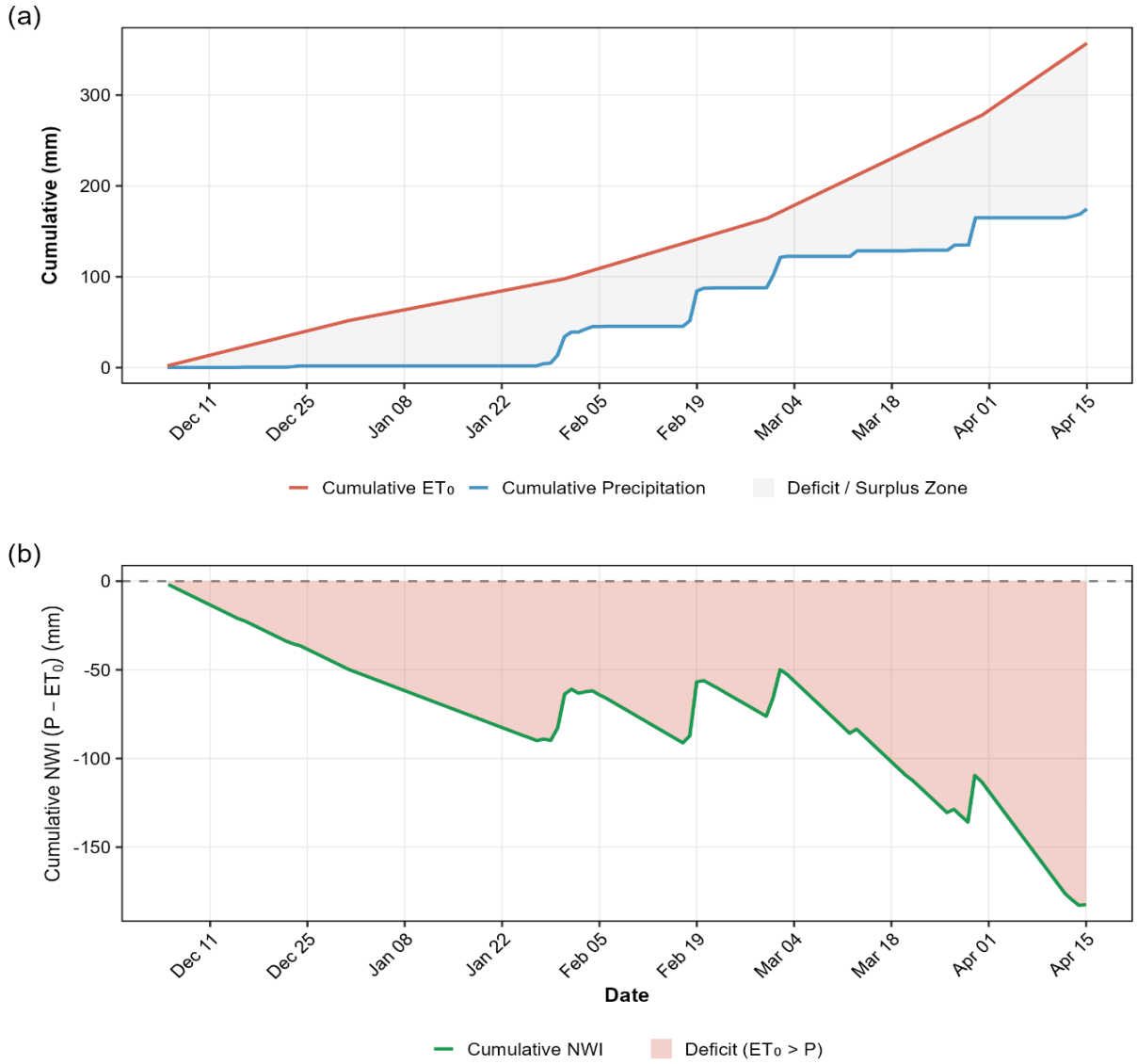

Figure 8: Cumulative Water Balance Components During the Monitoring Period. (a) Cumulative Reference Evapotranspiration and Cumulative Precipitation; (b) Cumulative Net Water Input

TDS Dynamics: During the initial equilibration period (December 5-12, 2023), marked by the yellow area in Figure 9, Total Dissolved Solids (TDS) concentrations varied widely, from approximately 600 to 2,160 mg/L. After the sudden increase in the water table on December 13, TDS concentrations rose sharply to around 3,000 mg/L and then gradually settled into the range of 3,300-3,500 mg/L until the end of January. Since February, TDS concentrations have been more variable, dropping temporarily to around 2,300-2,800 mg/L in response to large precipitation events (noting the February 18 event), before quickly returning to 3,000-3,900 mg/L.

DOI: https://doi.org/10.57041/f3yffx28

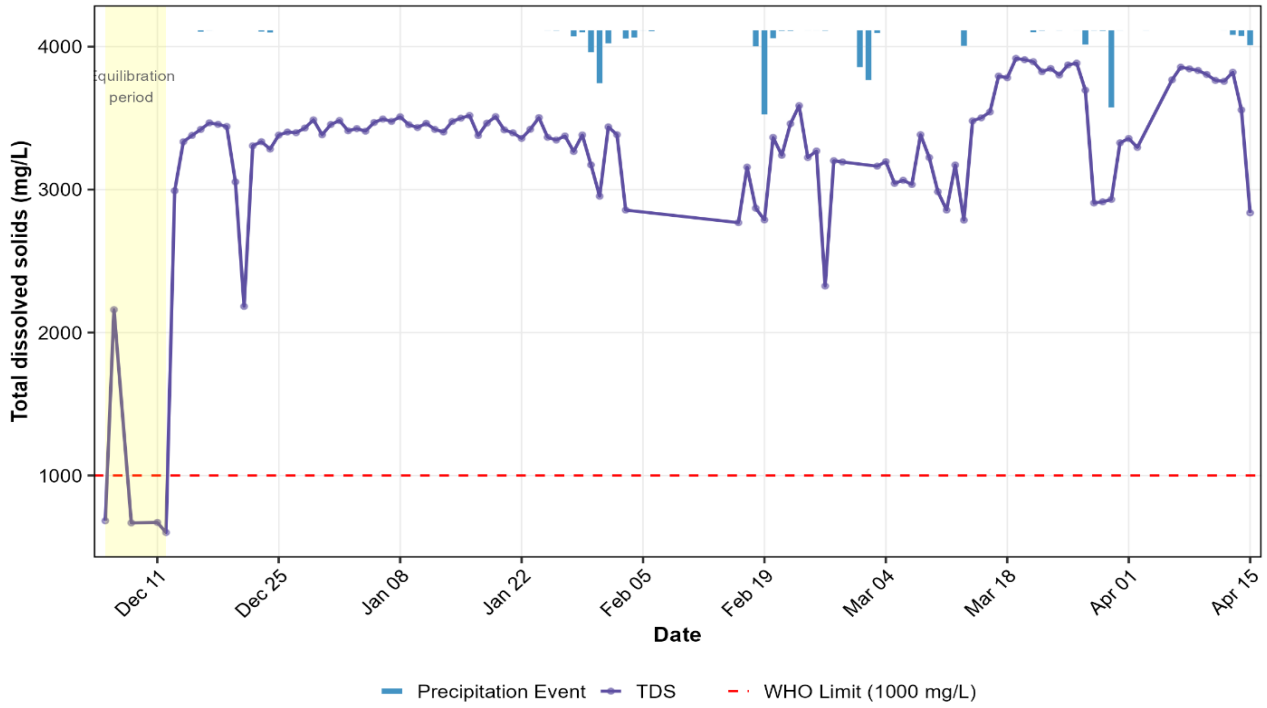

Figure 9: Time Series of Total Dissolved Solids (TDS) Concentration at the Monitoring Well

Note: Light blue bars indicate daily precipitation. The dashed red line denotes the WHO guideline limit (1,000 mg/L), and the yellow-shaded region

The steady TDS values, which ranged from 2,800 to 3,900 mg/L, are higher than the World Health Organization's guideline value of 1,000 mg/L by a factor of three to four (as shown by the dashed red line in Figure 9). Although heavy precipitation events led to temporary decreases in TDS, these values returned to normal, implying that the dissolved-solids pool in the aquifer is restored to its normal state.

Monthly Summary: The average groundwater level showed a steady rise from approximately 54.8 ft in December 2023 to about 57.0 ft in the initial part of April 2024. The rate of deepening picked up from about 0.5 ft/month in January-February to around 1.2 ft/month in March, which corresponded to large increases in mean evapotranspiration (ET_0) and air temperature (ET_0 rising from 1.69 mm/day in January to 3.98 mm/day in March). The distribution in December has the largest variability, which is due to the first adjustment phenomenon, while the distribution in April is the most compact.

The NWI continued to be negative for each month, with the weakest deficit of -9.3 mm in February, where high precipitation events helped to offset evapotranspiration losses. The deficit was highest in April, with -67.6 mm over 15 days, reflecting rising temperatures and high evapotranspiration rates in the absence of high precipitation events. These variations thus define a water deficit season that causes progressive aquifer depletion in the absence of constant managed aquifer recharge (MAR) system operation.

Table 2: Monthly Summary of Groundwater Depth and Hydroclimatic Parameters

Month	Mean GW Depth (ft)	ΔGW (ft)	Total Precip. (mm)	Mean ET_0 (mm/day)	Total ET_0 (mm)	NWI (mm)
Dec 2023	54.8	–3.94*	1.80	1.87	50.5	–48.7
Jan 2024	54.5	+1.07	32.25	1.69	52.4	–20.2
Feb 2024	55.5	+0.49	54.62	2.21	63.9	–9.3
Mar 2024	56.4	+1.23	93.24	3.98	123.4	–30.2
Apr 2024 (1–15)	57.0	+0.31	9.68	5.15	77.3	–67.6

**ΔGW: Change in monthly mean groundwater depth relative to the previous month. Deepening (decrease in the water table) is indicated by positive readings .Includes the sudden initial change that occurred on December 12–13.= Net Water Input.*

DOI: https://doi.org/10.57041/f3yffx28

Precipitation Event Response Analysis: Over the course of the monitoring period, seven different precipitation events were identified, each of which produced cumulative rainfall of more than 1 mm. The size of the events ranged from 1.3 mm (Event 1, 23 December) to 43.6 mm (Event 2, 25 January), with four events exceeding 30 mm (Events 2, 3, 4, and 6). The groundwater level was recorded from three days before each event to 15 days after the onset of each precipitation event.

The faceted plots (Figure 10) suggest that the larger events (>30 mm) were associated with the greater water-table response, although none of the events caused a clear, sustained rise in the water table. Events that occurred when the water table was shallow (December-January) were associated with greater dynamic fluctuations than similar events that occurred when the water table was deep (March-April), as expected due to the greater thickness of the vadose zone, which has served to reduce and delay the recharge signal. There has been little or no response associated with the smaller events (<10 mm).

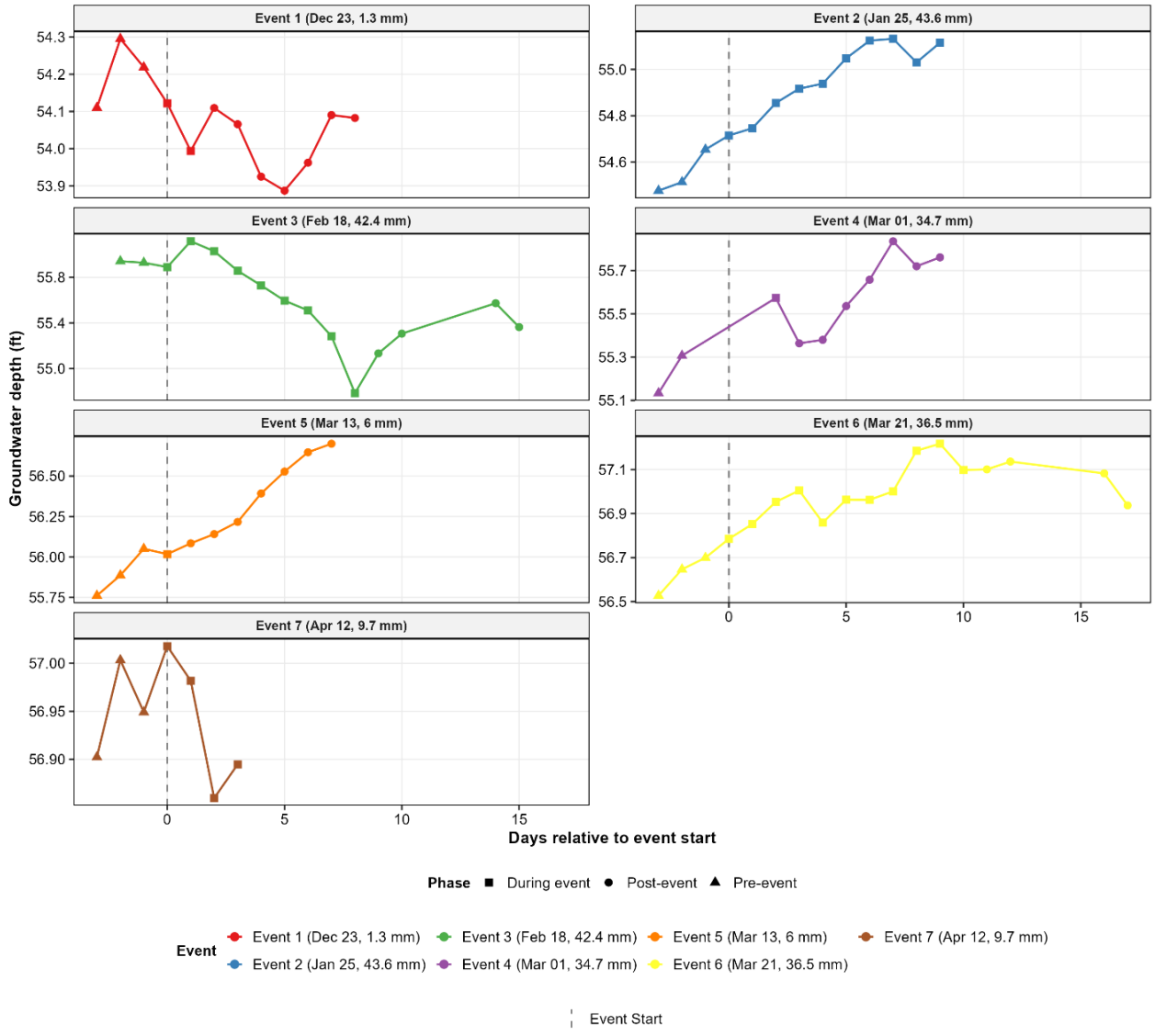

Figure 10: Faceted Event-Response Plots Showing Groundwater Depth Before, During, and After Seven Precipitation Events

Note: Each panel is labeled with the event date and cumulative rainfall. Marker shapes distinguish pre-event (triangles), during-event (squares), and post-event (circles) phases. The dashed vertical line marks the event onset.

DOI: https://doi.org/10.57041/f3yffx28

DISCUSSION

Performance of the IoT-Based Monitoring System: The results of laboratory calibration and field testing indicate that the low-cost IoT-based monitoring system is capable of providing accurate and continuous groundwater level data with a level of accuracy comparable to that of the commercial HOBO U20L sensor. The calibration curve describing the relationship between voltage and depth has a high coefficient of determination ($R^2 = 0.9982$), and there is a strong level of agreement between the smart system and HOBO sensor data during dynamic validation testing (RMSE ≈ 2.83 cm).

The IoT network provides a number of benefits over traditional monitoring methods, such as real-time data transfer, uninterrupted high-frequency data collection, low unit cost (compared to commercial HOBO sensors), and remote access. Taken together, these aspects make it easier to avoid frequent site visits and quickly identify unusual groundwater conditions (Jadoon *et al*., 2023). However, many limitations were noted throughout the investigation, including the data gap brought on by the solar charge controller's failure and the consistent, stable temperature readings that raise the possibility of sensor malfunction or software issues.

There have been other reports of comparable IoT-based groundwater monitoring solutions. For instance, low-cost Arduino-based systems have been effectively used for environmental monitoring in general (e.g., Pérez-Expósito *et al*., 2017) and water level monitoring in India (e.g., Kumar *et al*., 2020). By demonstrating the suitability of such systems for Managed Aquifer Recharge (MAR) wells in the hydrogeological and climatic settings of South Asia, this work adds to the body of research.

Hydroclimatic Factors Controlling Groundwater Dynamics: The findings indicate that while precipitation has a comparatively smaller impact than anticipated, evapotranspiration and air temperature are the main variables influencing groundwater level. Precipitation and groundwater level did not statistically significantly correlate on a daily basis. On a daily basis, however, reference evapotranspiration and air temperature demonstrated substantial positive associations with groundwater level, suggesting that the observed water table reduction is mostly due to high atmospheric demand during the winter-spring transition. In contrast to the expected rapid 1-3 day response characteristic of sites with shallower water tables or preferential flow paths, cross-correlation analysis shows that the strongest negative correlation between precipitation and groundwater level occurs at a 7-day lag. This reflects the delayed recharge response consistent with the thick (~54-58 ft) vadose zone at the site.

The water balance regression study, which revealed that NWI only accounted for 2% of the fluctuation in ΔGW on a weekly timeline, further supports ET_0's supremacy in this process. This shows that the processes governing the short-term dynamics of groundwater levels are not sufficiently described by the surface water balance model. This is probably because lateral groundwater flow, the time lag in vadose zone transmission, and local extraction are ignored. The findings of Wu *et al*. (2020) and Green *et al*. (2011), who demonstrated that higher atmospheric demand results in a decrease in soil moisture available for recharge, are in line with the positive correlation between ET_0 and groundwater level. ET_0 has a more significant role in regulating net recharge in semi-arid metropolitan locations like Islamabad, where impermeable surfaces worsen the impact of infiltration (Basharat and Tariq, 2013).

Implications for Managed Aquifer Recharge (MAR) in Islamabad: The cumulative Net Water Imbalance (NWI) was negative throughout the period of this study, with a value of about -180 mm by mid-April. This means that precipitation alone is not sufficient to balance the losses of evapotranspiration during the dry season of winter and spring, and is not able to compensate for groundwater extraction. The cumulative water balance shows that the accumulated value of evapotranspiration (ET_0) of about 350 mm was twice the value of accumulated precipitation of about 170 mm. Taken together, these findings suggest that the operation of managed aquifer recharge (MAR) would be most beneficial during the monsoon season (July to September), when the precipitation surplus is available, while the dry season examined in this study represents the period of maximum aquifer stress when additional recharge is required.

The concentrations of dissolved solids (TDS) varied between 2,300 and 3,900 mg/L after equilibration (Figure 8) and were always higher than the World Health Organization's recommended value of 1,000 mg/L by a factor of 3-4. Although there were instances where TDS decreased temporarily after heavy precipitation events (for example, the event of February 18, where 42.4 mm of precipitation caused a temporary decrease in TDS to ≈2,300 mg/L), the values increased rapidly, suggesting that the aquifer matrix controls the budget of dissolved solids. TDS and groundwater depth had a weak association, according to the correlation matrix. The necessity of water quality monitoring during Managed Aquifer Treatment is shown by the elevated TDS readings. Prior to the recharged water being fit for human consumption, it is necessary to look into the mineralogical origins of dissolved solids.

Limitations and Future Research: It is important to note some of this study's shortcomings. First off, the monsoon recharge season, which is crucial, was not included in the monitoring period (December 2023–April 2024), which only covered the dry season. A full year is needed to evaluate the MAR system thoroughly. Second, in-situ

observations from Pakistan Meteorological Department sites may be more accurate than satellite-derived hydroclimatic data (NASA POWER). Thirdly, the low R2 value (0.02) of the water balance equation could have been caused by runoff, lateral flow, abstraction by neighboring wells, and changes in soil moisture, all of which are not taken into consideration by the water balance equation ($P - ET_0$).

Future studies should address these limitations by including monitoring periods of at least one year, using ground-based meteorological data, using improved temperature sensors for thermal tracer studies, and using numerical groundwater flow models to better separate the recharge and discharge terms. Additionally, the use of multiple IoT monitoring networks in the Islamabad MAR well network would allow for the spatial analysis of recharge heterogeneity and its association with the local hydrogeology.

Conclusions: This is the first recorded use of a low-cost, Internet of Things (IoT)-aided groundwater level measurement system in a managed aquifer recharge (MAR) well in Islamabad, Pakistan. The results showed that the IoT system was accurate to the same level as the commercial HOBO U20L water level sensor (RMSE = 2.83 cm; $R^2 = 0.9982$; NSE = 0.9981) but at a much lower cost, with the additional benefit of real-time data transfer. Over the period of groundwater level monitoring from December 2023 to April 2024, the water table decreased by about 3 feet, mainly due to evapotranspiration (daily correlation with groundwater level: $r = 0.703$, $p < 0.001$) and not due to precipitation deficits (daily correlation: $r = 0.133$, $p = 0.162$). The lagged cross-correlation analysis indicated an optimal lag of 7 days between precipitation and groundwater level ($r = -0.474$), which is consistent with the attenuation effect of the thick vadose zone.

Throughout the monitoring period, the cumulative water balance revealed a consistent deficit of roughly -180 mm, indicating that precipitation during the dry season is insufficient to sustain groundwater levels. With relatively brief drops following significant storm events, the total dissolved solids (TDS) levels were found to be three to four times higher than the World Health Organization's (WHO) recommended value of 1,000 mg/L. Only 2% of the variation in groundwater level variations could be described by weekly net water input ($R^2 = 0.02$, $p = 0.59$), indicating that other processes, including abstractions, delayed transmission, and lateral movement, are also crucial. When combined, these findings lend credence to the necessity of year-round Internet of Things monitoring, the incorporation of water quality variables into managed aquifer recharge (MAR) management, and a more extensive implementation of MAR systems in Pakistan.

Acknowledgments The authors give credit to Dr. Khan Zaib Jadoon and associates for the concept and original design of the Internet of Things-based smart groundwater monitoring system (Jadoon *et al*., 2023). They are also acknowledged for providing access to the managed aquifer recharge (MAR) well site.

REFERENCES

Arshad, M., Iqbal, N., and Ashraf, M. (2023). From Crisis to Sustainability: Managing Aquifer Recharge in Pakistan. Pakistan Council of Research in Water Resources (PCRWR), Islamabad, 61 pp.

Basharat, M., and Tariq, A.-u.-R. (2013). Spatial climate variability and its impact on irrigated hydrology in a canal command. Arabian Journal for Science and Engineering, 38(3), 507–522.

Bates, B., Kundzewicz, Z.W., Wu, S., and Palutikof, J. (2008). Climate Change and Water. Technical Paper of the Intergovernmental Panel on Climate Change, IPCC Secretariat, Geneva.

Bhatti, M.T., Anwar, A.A., and Aslam, M. (2017). Groundwater monitoring and management: Status and options in Pakistan. Computers and Electronics in Agriculture, 135, 143–153.

Condon, L., Kollet, S., Bierkens, M.F.P., Fogg, G.E., Maxwell, R.M., Hill, M.C., *et al*. (2021). Global groundwater modeling and monitoring: Opportunities and challenges. Water Resources Research, 57, e2020WR029500.

Daliakopoulos, I.N., Coulibaly, P., and Tsanis, I.K. (2005). Groundwater level forecasting using artificial neural networks. Journal of Hydrology, 309(1), 229–240.

Dillon, P. (2005). Future management of aquifer recharge. Hydrogeology Journal, 13(1), 313–316.

Dillon, P., Stuyfzand, P., Grischek, T., Lluria, M., Pyne, R.D.G., Jain, R.C., *et al*. (2019). Sixty years of global progress in managed aquifer recharge. Hydrogeology Journal, 27(1), 1–30.

Famiglietti, J.S. (2014). The global groundwater crisis. Nature Climate Change, 4(11), 945–948.

Gorelick, S.M., and Zheng, C. (2015). Global change and the groundwater management challenge. Water Resources Research, 51(5), 3031–3051.

Green, T.R., Taniguchi, M., Kooi, H., Gurdak, J.J., Allen, D.M., Hiscock, K.M., *et al*. (2011). Beneath the surface of global change: Impacts of climate change on groundwater. Journal of Hydrology, 405(3), 532–560.

IAH (International Association of Hydrogeologists). (2017). Essential Indicators for Groundwater. IAH Strategic Overview Series.

Iqbal, M., Naeem, U.A., Ahmad, A., Ghani, U., and Farid, T. (2020). Relating groundwater levels with meteorological parameters using ANN technique. Measurement, 166, 108163.

Iqbal, N., Arshad, M., Bashir, A., and Piracha, A. (2023). Hydrological Assessment of Surface and Groundwater Resources of Islamabad, Pakistan. Pakistan Council of Research in Water Resources (PCRWR), Islamabad.

Jadoon, K.Z., Ali, M.Z., Yousafzai, H.U.K., Rehman, K.U., Shah, J.A., and Shiekh, N.A. (2023). Smart Groundwater Monitoring System for Managed Aquifer Recharge Based on Enabled Real-Time Internet of Things. EGU General Assembly 2023, Vienna, Austria, 24–28 April 2023, EGU23-12909.

Kumar V., Bharanidharan N., Bharanidharan S., Vanaja C. (2020). IoT Based Water Level Meter for Alerting Population about Floods. International Journal of Trend in Scientific Research and Development (IJTSRD), 4(6), 200–202.

Penman, H.L. (1948). Natural evaporation from open water, bare soil and grass. Proceedings of the Royal Society of London. Series A, 193, 120–145.

Pérez-Expósito, A. J., *et al*. (2017). VineSens: An IoT-based system for vineyard and environmental monitoring.

Qureshi, A.S. (2020). Groundwater governance in Pakistan: From colossal development to neglected management. Water, 12(11), 3017.

Qureshi, A.S., McCornick, P.G., Qadir, M., and Aslam, Z. (2008). Managing salinity and waterlogging in the Indus Basin of Pakistan. Agricultural Water Management, 95(1), 1–10.

Razzaq, A., Rehman, A., Qureshi, A.H., Javed, I., Saqib, R., and Khan, I. (2022). Analyzing past and future trends in Pakistan's groundwater irrigation development: Implications for environmental sustainability and food security. Environmental Science and Pollution Research, 30, 35413–35429.

Sophocleous, M. (2004). Global and regional water availability and demand: Prospects for the future. Natural Resources Research, 13(2), 61–75.

Todd, D.K., and Mays, L.W. (2005). Groundwater Hydrology, 3rd ed. John Wiley & Sons, Hoboken, NJ.

United Nations. (2022). UN World Water Development Report 2022: Groundwater – Making the Invisible Visible. UNESCO, Paris.

WHO (World Health Organization). (2017). Guidelines for Drinking-water Quality, 4th ed. incorporating the 1st addendum. WHO, Geneva.

Wu, W.-Y., Lo, M.-H., Wada, Y., Famiglietti, J.S., Reager, J.T., Yeh, P.J.-F., *et al*. (2020). Divergent effects of climate change on future groundwater availability in key mid-latitude aquifers. Nature Communications, 11(1), 3710.

Zhang, H., Xu, Y., and Kanyerere, T. (2020). A review of the managed aquifer recharge: Historical development, current situation and perspectives. Physics and Chemistry of the Earth, Parts A/B/C, 118–119, 102887.